Rare Metal Materials and Engineering
Volume 54, Issue 10, October 2025
Available online at www.rmme.ac.cn

Science Press

Cite this article as: Wang Rui, Li Jiarong, Yue Xiaodai, et al. Microstructure Evolution During Creep of Single Crystal Superalloy DD9[J]. Rare Metal Materials and Engineering, 2025, 54(10): 2445-2452. DOI: https://doi.org/10.12442/j.issn.1002-185X.20240540.

ARTICLE

Microstructure Evolution During Creep of Single Crystal Superalloy DD9

Wang Rui, Li Jiarong, Yue Xiaodai, Zhao Jinqian, Yang Wanpeng

Science and Technology on Advanced High Temperature Structural Materials Laboratory, Beijing Institute of Aeronautical Materials, Beijing 100095, China

Abstract: Interrupted and ruptured creep tests were conducted on single crystal superalloy DD9 at 980 °C/250 MPa and 1100 °C/137 MPa conditions. Microstructure evolution during creep was analyzed through scanning electron microscope and transmission electron microscope. Results show that the microstructure evolutions are similar under the creep conditions of 980 °C/250 MPa and 1100 °C/137 MPa. Cubical γ' phase, which is dispersedly distributed in the γ matrix, gradually evolves into a layered structure perpendicular to the stress direction. The width of the γ matrix channel along the direction parallel to the stress increases. The relationship between the increase in width of the γ matrix channel and the strain satisfies linear relationship in logarithmic form, indicating that the width of the γ matrix can be deduced via the strain under creep state. This may provide an approach to investigate the width of γ matrix in single crystal superalloys during creep under high temperature and low stress conditions. In the early creep stage, dislocations formed in the γ phase generate mutually perpendicular networks through cross-slip at the γ/γ' interface. Then, stable hexagonal dislocation networks form as a result of the coupling effects of external stress and mismatch stress at high temperatures. In the later period of creep, dislocations shear the γ' phase, ultimately causing the fracture.

Key words: single crystal superalloy; DD9; creep; microstructure evolution; dislocations

1 Introduction

Nickel-based single crystal superalloys are preferred materials for the preparation of advanced aero-engine turbine blades due to their excellent comprehensive properties[1–3]. Turbine blades are subjected to huge centrifugal force when operated at high temperature, which can cause creep damage to the single crystal superalloys. Thus, creep properties of single crystal superalloys are important factors affecting the reliability of aero-engines. For single crystal superalloys, their creep performance is closely related to the microstructure[4–13]. Evolution of microstructures of single crystal superalloys occurs under service environment, which can directly affect the creep properties. Therefore, it is of great significance to study the microstructure evolution during creep process of single crystal superalloys and to provide a theoretical reference for the design and application of single crystal superalloys.

The influence factors, such as chemical composition and crystal orientation, affecting creep properties of single crystal superalloys attract widespread attention. Li et al[4] studied the effect of the alloying element rhenium on the creep rupture life of a single crystal superalloy. Chen et al[10] analyzed the effect of the content of Mo, W, and Ti on creep properties of single crystal superalloys. Wang et al[14–15] investigated the effect of orientation on creep properties of DD6 alloy at 760 and 980 °C. Hu et al[7] analyzed the single crystal superalloy with <111> misorientation to study the effect of small angle deviation from <111> on the creep properties of single crystal superalloy. Shi et al[16] studied the creep properties of [001], [011], and [111] orientations of DD15 alloy to analyze the creep anisotropy. Many researchers focus on the microstructure evolution during creep process of single crystal superalloys. Dislocation behavior[17–21] during creep process is the main research interest, which includes two aspects: (1) the mechanisms of dislocations shearing γ' phase under low temperature and high stress; (2) the evolution of dislocation networks under high temperature and low stress. However,

Received date: October 20, 2024
Corresponding author: Li Jiarong, Ph. D., Professor, Science and Technology on Advanced High Temperature Structural Materials Laboratory, Beijing Institute of Aeronautical Materials, Beijing 100095, P. R. China, Tel: 0086-10-62497202, E-mail: jrli126@126.com

few researches[22] reported the evolution of γ and γ' phases.

In this research, the evolution of microstructure in a third-generation single crystal superalloy DD9 during creep process was investigated to provide theoretical support for the design and application of the third-generation single crystal superalloy.

2 Experiment

The third-generation single crystal superalloy DD9 was used in this research. The composition of superalloy DD9 is 3.5Cr-7Co-2Mo-6.5W-7.5Ta-4.5Re-0.5Nb-5.6Al-0.1Hf-0.008C-0.001Y-Ni (wt%)[23–24]. [001]-oriented samples with diameter of 15 mm and length of 200 mm were cast by the seed crystal method of investment casting. The as-cast samples were then used for heat treatment: pre-heat treatment+1340 °C/6 h/air cooling+1140 °C/6 h/air cooling+870 °C/32 h/air cooling. Afterwards, the samples were machined for creep tests. The schematic diagram of DD9 sample for creep test is shown in Fig.1.

Interrupted and ruptured creep tests at 980 °C/250 MPa and 1100 ° C/137 MPa conditions were conducted. For the interrupted creep test, the creep tests were interrupted when the strain reached 0.2%, 0.5%, 1.0%, and 2.0%. The interrupted samples were taken for cross-section observation to analyze the microstructure, and the sampling position is shown in Fig.2. The samples taken from A-A and B-B sections were ground, polished, and etched in chemical reagent (200 mL H_2O+160 mL HCl+50 g $CuSO_4$+10 mL H_2SO_4). ZEISS Sigma 300 field-emission scanning electron microscope (SEM) was used to observe the microstructure of the etched samples. At least 6 dendrite regions were randomly selected and then observed by SEM for statistic analysis of the γ channel width.

A thin sheet with thickness of 0.4 mm was taken from B-B section, ground into a sheet with thickness of <50 μm, and then punched into a round sheet with diameter of 3 mm for electrolytic double spraying through electrolyte of 10vol% $HClO_4$ ethanol solution to prepare thin area. The dislocation configuration in the thin area was observed by Tecnai G^2 F20 transmission electron microscope (TEM).

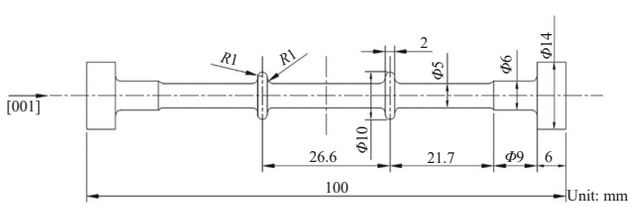

Fig.1 Schematic diagram of DD9 sample for creep test

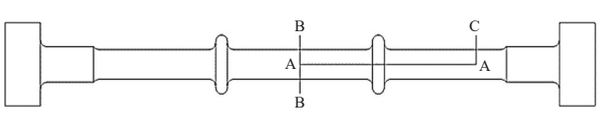

Fig.2 Schematic diagram of sampling position after interrupted creep tests

3 Results

3.1 Microstructure before creep process

The microstructures of DD9 sample before creep test are presented in Fig.3. Cubic γ' phases are uniformly dispersed in the γ matrix, and the average γ channel width is 0.05 μm. As shown in Fig.3b, dislocation lines cannot be observed.

3.2 Microstructure evolution during creep process

Fig.4 shows the creep curves of DD9 samples under 980 °C/250 MPa and 1100 ° C/137 MPa conditions, which also presents the locations of interrupted (strain of 0.2%, 0.5%, 1.0%, and 2.0%) and ruptured points. The creep curve of DD9 sample at 1100 ° C/137 MPa is similar to that of the third-generation single crystal superalloy TMS-75[25].

Fig. 5 shows 3D microstructures of DD9 samples under 980 ° C/250 MPa condition. At strain of 0.2%, directional coarsening of γ' phase, namely rafting, in some areas occurs along the direction perpendicular to the stress direction. The γ' phase in most regions is not rafted. At strain of 0.5%, all γ' phases develop into the raft shape. Partial matrix channel parallel to the stress direction is blocked by γ' phase when the strain increases to 1.0%, which indicates that γ' phases are connected along the stress direction. The degree of γ' phase connectivity further increases at strain of 2.0%. The width of γ matrix channel increases obviously. The γ' phase along the stress direction and the γ/γ' interface become irregular after rupture.

3D microstructures of DD9 sample during creep process under 1100 °C/137 MPa condition are shown in Fig.6. The γ' phase evolves into a raft at strain of 0.2%. When the strain is 0.5%, γ' phase keeps a raft shape. Connection between γ' phases occurs at strain of 1.0%. The degree of connection

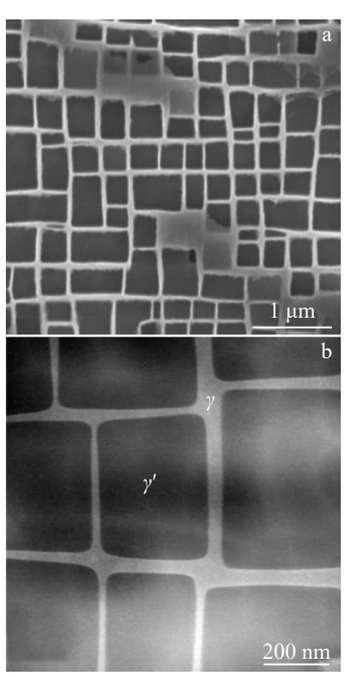

Fig.3 SEM (a) and TEM (b) microstructures of DD9 sample before creep test

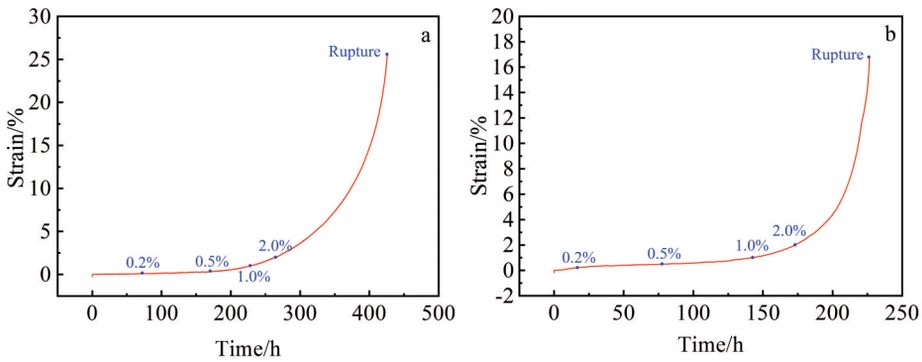

Fig.4 Creep curves of DD9 samples under 980 °C/250 MPa (a) and 1100 °C/137 MPa (b) conditions

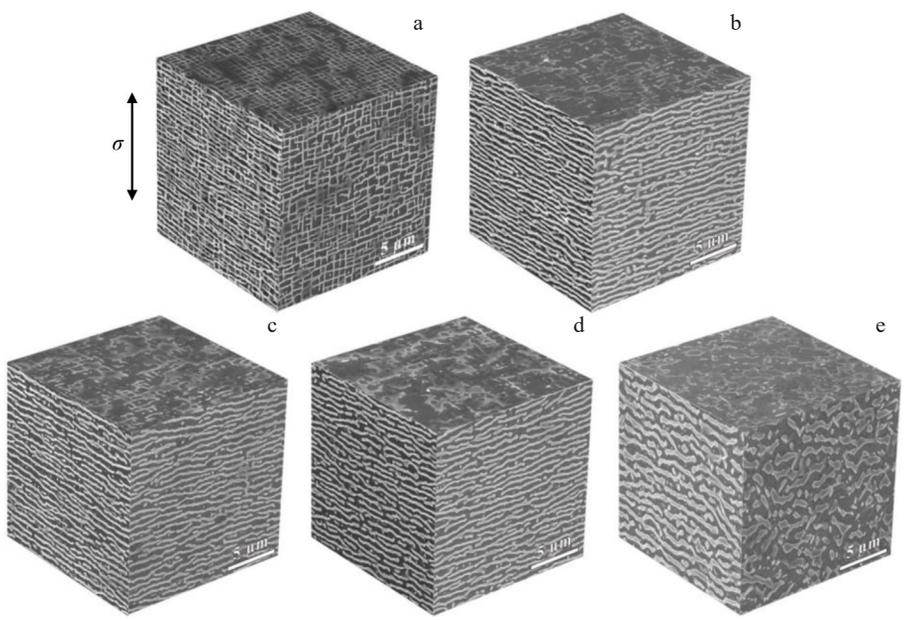

Fig.5 3D microstructures of DD9 sample during creep process under 980 °C/250 MPa condition: (a) strain=0.2%; (b) strain=0.5%; (c) strain=1.0%; (d) strain=2.0%; (e) rupture

further increases at strain of 2.0%. After rupture, the width of the γ matrix channel and γ' phase becomes quite large, and the shape of γ and γ' phases becomes irregular.

The microstructure evolutions of DD9 alloy during creep process under 1100 °C/137 MPa and 980 °C/250 MPa conditions are similar. The width of both the γ matrix channel and the γ' phase increases. Therefore, the planes perpendicular to the stress direction, namely (001) planes, show the flaky structure of γ' and γ phases in Fig. 5 and Fig. 6, respectively. The formation of the flaky structure perpendicular to the stress direction results from the negative γ/γ' lattice mismatch under tensile stress[26]. The γ/γ' lattice mismatch of DD9 alloy is negative, which is similar to that of the other third-generation single crystal superalloys[27–28]. Similar microstructure evolutions also occur in TMS-75 alloy[25,29] and DD33 alloy[28] during creep process under high temperature and low stress conditions.

The movements of dislocations mainly involve the γ matrix during creep process of single crystal superalloys under high temperature and low stress conditions[30]. Therefore, the width of the γ matrix channel has a significant effect on the movement of dislocations, which also affects the mechanical properties of alloys[31]. Fig. 7 shows the variation in width of the γ matrix channel under different conditions. The width of the γ matrix channel is increased with the increase in creep deformation. However, the increasing rate gradually slows down. Alexander et al[32] analyzed the evolution of the width of γ matrix channel over time during creep process of CMSX-4 alloy. They assumed that the increasing rate of width could be divided into two stages through the parameter $3w_0$, where w_0 is the initial width of the γ matrix channel. This increasing mode of the width of γ matrix channel is different from that in this research.

The movement of dislocations during creep generates a significant impact on the creep behavior of single crystal superalloys. Inhibiting the movement of dislocations can effectively reduce the creep rate and eventually improve creep life for single crystal superalloys[33–34].

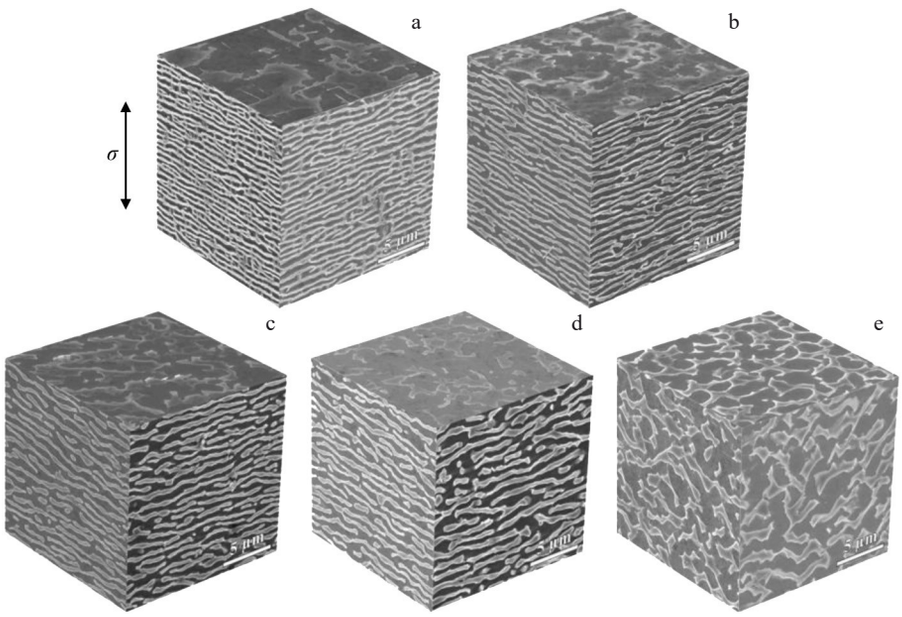

Fig.6 3D microstructures of DD9 sample during creep process under 1100 °C/137 MPa condition: (a) strain=0.2%; (b) strain=0.5%; (c) strain=1.0%; (d) strain=2.0%; (e) rupture

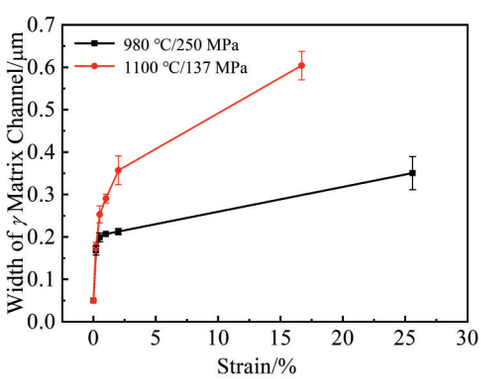

Fig.7 Evolution of the width of γ matrix channel during creep under different conditions

Fig. 8 shows the evolution of dislocation configurations of DD9 sample under 980 °C/250 MPa condition. Dislocation networks exist in intersecting form accompanied by dislocation bowing at strain of 0.2% (Fig. 8a). At strain of 0.5%, dislocation networks change into wave form, resulting from dislocation reactions (Fig. 8b). No obvious transformation of dislocation networks occurs at strain of 1.0% (Fig. 8c), compared with the microstructure at strain of 0.5%. Dislocation networks evolve into the hexagon shape at strain of 2.0% (Fig.8d).

Fig. 9 shows the evolution of dislocation configurations of DD9 sample under 1100 °C/137 MPa condition. It is demonstrated that the dislocation networks are gradually transformed into wave form (Fig. 9a). At strain of 0.5%, the dislocation networks change completely into wave form and remain the wave form at strain of 1.0%. At strain of 2.0%, dislocation networks develop into the hexagon shape (Fig.9d), which is similar to situation under 980 °C/250 MPa condition.

These phenomena (dislocation morphology and evolution process) have already been reported in other researches[25,35–36]. Considerable slip systems are activated during creep under high temperature and low stress conditions, and the deformation is mainly caused by dislocation movement within the γ matrix. Dislocations slipping towards different directions encounter the γ/γ' interface, forming dense dislocation networks.

4 Discussions

4.1 Evolution of γ' and γ phases

During creep process of DD9 sample, γ' phase experiences the rafting-derafting process, as shown in Fig. 5 and Fig. 6. Furthermore, at the same strain, the evolution degree of γ' phase under 1100 °C/137 MPa condition is greater than that under 980 °C/250 MPa condition. The morphology evolution of γ' phase is essentially caused by the diffusion of elements, which is a thermally activated process[37]. Therefore, the increase in creep temperature from 980 °C to 1100 °C can promote the morphology evolution of the γ' phase. In addition, increasing the creep stress can also accelerate the morphology evolution of γ' phase[38–39]. Evolution degree of microstructure under 1100 °C/137 MPa condition is greater than that under 980 °C/250 MPa condition, suggesting that the promotion effect caused by temperature increase is more pronounced than the retardation effect of stress decrease on the morphology evolution of γ' phase in this research.

It is indicated that dislocation movements mainly occur in γ matrix, as shown in Fig.8 and Fig.9. The increase in width of γ matrix channel may affect the mechanical properties of alloys[40], so it is important to investigate the increasing law of the width of γ matrix channel. The curves in Fig. 7 can be

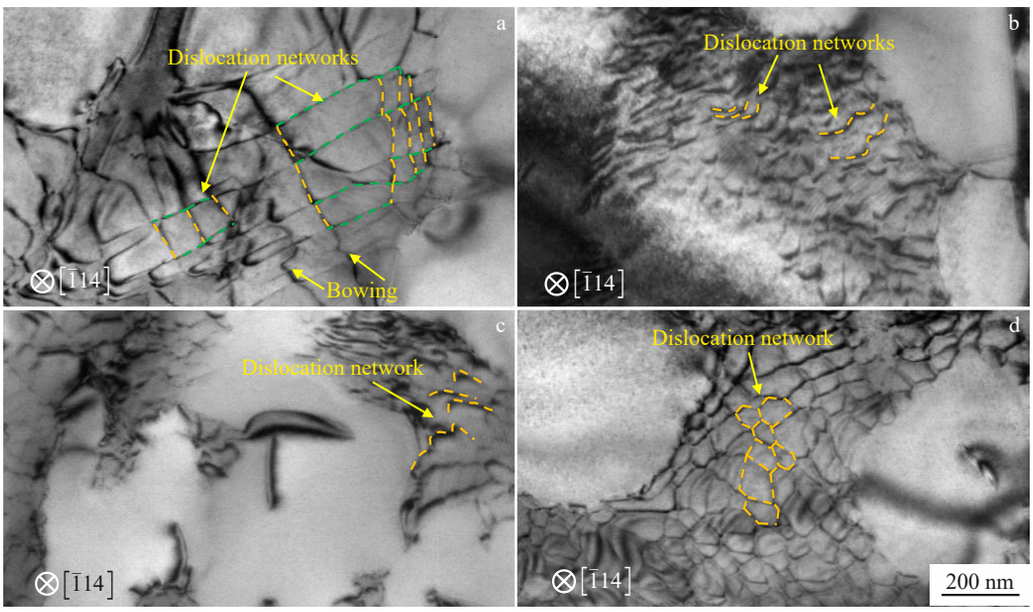

Fig.8 Dislocation configurations of DD9 sample during creep process under 980 °C/250 MPa condition: (a) strain=0.2%; (b) strain=0.5%; (c) strain=1.0%; (d) strain=2.0%

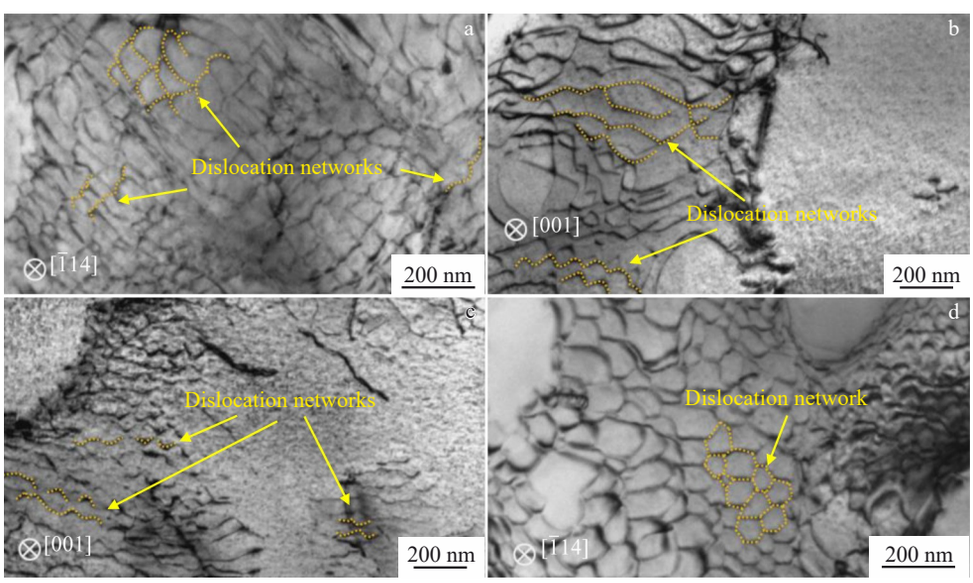

Fig.9 Dislocation configurations of DD9 sample during creep process under 1100 °C/137 MPa condition: (a) strain=0.2%; (b) strain=0.5%; (c) strain=1.0%; (d) strain=2.0%

transformed into different forms, as shown in Fig. 10. Δw is the width increment of the γ matrix channel, and it is calculated by Eq.(1), as follows:

$$\Delta w = w_{\varepsilon} - w_0 \quad (1)$$

where ε is strain; w_{ε} is the width of γ matrix channel at the strain ε; w_0 is the initial width of γ matrix channel (0.05 μm).

The results in Fig. 10a – 10b demonstrate the linear relationships between lgΔw and lgε under 980 °C/250 MPa and 1100 °C/137 MPa conditions, respectively. The fitting curves indicating the relationship between Δw with ε under 980 °C/250 MPa and 1100 °C/137 MPa conditions are shown in Fig.10c and 10d, respectively, revealing that the fitting curves match well with the experimental data.

It can be concluded that the increasing mode of the width of γ matrix channel with strain of DD9 alloy during creep under high temperature and low stress conditions remains consistent throughout the creep process. This may be ascribable to the fact that the variations of diffusion rates for alloying elements are relatively stable with the increase in strain. However, two types of increasing modes of the width of γ matrix with the prolongation of creep time in CMSX-4 alloy during creep under high temperature and low stress conditions were reported in Ref.[32]. Therefore, using strain as the indication of the width of γ matrix channel or even the γ and γ' evolution

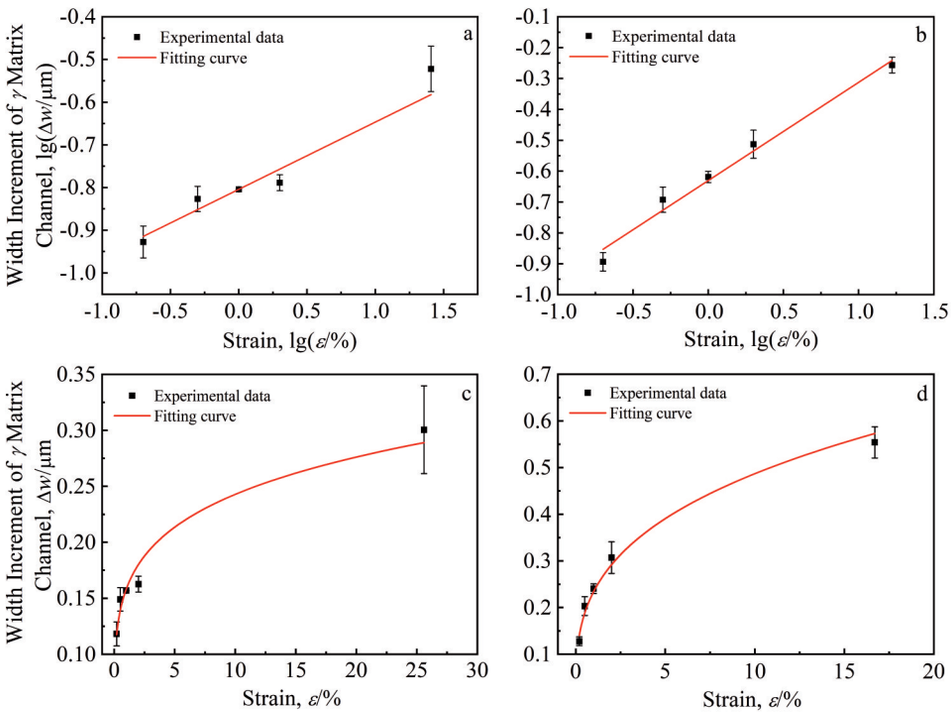

Fig.10 Different forms of relationship between width increment of γ matrix channel and strain ε under 980 °C/250 MPa (a, c) and 1100 °C/137 MPa (b, d) conditions: (a–b) lgΔw-lgε; (c–d) Δw-ε

during creep process of single crystal superalloys under high temperature and low stress conditions may be a suitable choice in practical engineering applications.

The morphology evolution of γ' and γ phases is essentially caused by the diffusion of alloying elements. The increase in width of the γ matrix channel infers the diffusion of γ phase-forming elements towards the γ phase and the γ' phase-forming elements towards the γ' phase. Under the coupling effects of creep stress and mismatch stress, directional diffusion of the alloying elements occurs, leading to the directional coarsening of γ' during creep process, i. e., along the direction perpendicular to the stress direction, as shown in Fig.5 and Fig.6.

The diffusion activation energy of the alloy is mainly related to the chemical composition and microstructure[37]. The chemical composition of the superalloy in this research is fixed, and the microstructures are affected by temperature and stress, indicating that the diffusion activation energy is mainly affected by temperature and stress. For single crystal superalloys, the effect of creep temperature on the evolution of microstructure is much greater than that of the creep stress[41–42]. Moreover, changing the temperature within a certain range cannot cause essential variation of the mechanism for directional mass diffusion[42–43]. Therefore, the deformation mechanisms of the alloy under these two conditions are similar, resulting in similar increasing laws of the width of γ matrix channel.

4.2 Evolution of dislocations

The evolutions of dislocation morphology of DD9 alloy during creep under 980 °C/250 MPa and 1100 °C/137 MPa conditions are quite similar. Under the effect of external stress, {111} <110> octahedral slip systems are prone to activation[37], leading to the formation of a/2<110> screw dislocations sliding on the {111} slip planes. These dislocations are blocked when encountering with γ/γ' interface, and then cross-slip occurs, leaving mutually perpendicular dislocation lines along the <110> direction[44], and thus generating the dislocation networks, as shown in Fig. 8a. The formation of <110> dislocation networks occurs in a very short time. The mutually perpendicular dislocation networks can only be observed at strain of 0.2% under 980 °C/250 MPa condition, as shown in Fig. 8a. As the creep process further proceeds, the mismatch between γ and γ' phases is reduced, which generates [010] edge misfit dislocations at the γ/γ' interface. These edge dislocations can maximize the reduction effect on mismatches[45]. The dislocations generated by creep stress and mismatch reduction encounter the <110> dislocation networks formed in the early stage of creep, forming <110>-<100> dislocation networks, and therefore presenting the wave form[30], as shown in Fig. 8b–8c and 9b–9c. Subsequently, the creep stress causes a further increase in the number of dislocations in γ phase, and the γ/γ' mismatch is further reduced to generate mismatch dislocations. The dislocations of two types react with the wave dislocation networks at γ/γ' interface, forming stable hexagonal dislocation networks[30,45], as shown in Fig. 8d and Fig. 9d. In general, the evolution of dislocation networks at γ/γ' interface is the result of coupling effects of external stress and mismatch stress under high temperature condition.

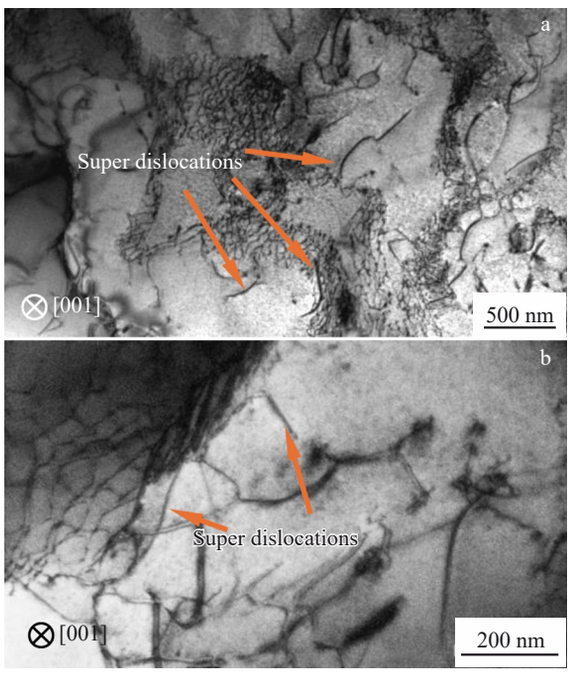

Fig.11 Dislocation configurations near creep fracture under different conditions: (a) 980 °C/250 MPa; (b) 1100 °C/137 MPa

It can be seen that stable dense dislocation networks form gradually at γ/γ' interface during creep process. Dislocation networks at γ/γ' interface can hinder the movement of newly generated dislocations[23], which results in the low creep rate during the steady creep stage of single crystal superalloys. In the later period of creep, the stress is increased because of the reduction of effective bearing area. Consequently, dislocations shearing the γ' phase increase gradually until fracture, as shown in Fig.11. The dislocation behavior of DD9 alloy under high temperature and low stress conditions are similar to that of other single crystal superalloys[10,45–46].

5 Conclusions

1) The cubical γ' phase dispersedly distributed in γ matrix gradually evolves into layered structure perpendicular to the stress direction, namely [001] orientation. The layered structure of γ' phase separates the γ matrix and shows rafting structure parallel to the (001) plane. The width of γ matrix channel along the stress direction is increased due to the directional diffusion of alloying elements.

2) The relationship between the width increment of γ matrix channel (Δw) and the strain (ε) during creep process under 980 °C/250 MPa and 1100 °C/137 MPa conditions satisfies linear relationship in logarithmic form, which indicates that the width increment of γ matrix channel may be inferred via the strain during creep process under high temperature and low stress conditions. Using strain as the indication of the width of γ matrix channel or even the γ and γ' evolution during creep process of single crystal superalloys under high temperature and low stress conditions may be a suitable choice in practical engineering applications.

3) In the early creep stage of DD9 alloy, dislocations forming in γ phase generate mutually perpendicular dislocation networks through cross-slip at γ/γ' interface. Then, stable hexagonal dislocation networks form. In the later period of creep process, dislocations shear γ' phase, ultimately causing the fracture.

References

1 Reed R C. *The Areonautical Journal*[J], 2006, 112(1131): 291
2 Pollock T M, Tin S. *Journal of Propulsion and Power*[J], 2006, 22(2): 361
3 Sato A, Chiu Y L, Reed R C. *Acta Materialia*[J], 2011, 59(1): 225
4 Li J R, Tang D Z, Lao R L *et al*. *Journal of Materials Science and Technology*[J], 1999, 15(1): 53
5 Wang Kaiguo, Li Jiarong, Cao Chunxiao. *Journal of Materials Engineering*[J], 2004, 32(1): 3 (in Chinese)
6 Shi Z X, Liu S Z, Wang X G *et al*. *Materials Science Forum*[J], 2015, 816: 513
7 Hu Bin, Li Shusuo, Pei Yanling *et al*. *Acta Metallurgica Sinica*[J], 2019, 55(9): 1204 (in Chinese)
8 Li Y F, Wang L, Zhang G *et al*. *Materials Science and Engineering A*[J], 2019, 760: 26
9 Zhang Z K, Wen Z X, Yue Z F. *Journal of Alloys and Compounds*[J], 2020, 851: 156767
10 Chen J B, Huo Q Y, Chen J Y *et al*. *Materials Science and Engineering A*[J], 2020, 799: 140163
11 Huang Y S, Wang X G, Cui C Y *et al*. *Journal of Materials Science and Technology*[J], 2021, 69: 180
12 Zeng Qiang, Chen Xuhui, Wu Baoping *et al*. *Rare Metal Materials and Engineering* [J], 2022, 51(9): 3394 (in Chinese)
13 Xiong Jiangying, Long Anping, Zhang Jianting *et al*. *Rare Metal Materials and Engineering*[J], 2021, 50(11): 3995 (in Chinese)
14 Wang Kaiguo, Li Jiarong, Liu Shizhong *et al*. *Journal of Materials Engineering*[J], 2004, 32(5): 7 (in Chinese)
15 Wang Kaiguo, Li Jiarong, Liu Shizhong *et al*. *Journal of Materials Engineering*[J], 2004, 32(8): 7 (in Chinese)
16 Shi Z X, Liu S Z, Yue X D *et al*. *Rare Metal Materials and Engineering*[J], 2022, 51(10): 3542
17 Agudo J L, Nörtershäuser P, Somsen C *et al*. *Acta Materialia*[J], 2014, 69(1): 246
18 Ru Y, Li S S, Zhou J *et al*. *Scientific Reports*[J], 2016, 6: 29941
19 Wu X X, Wollgramm P, Somsen C *et al*. *Acta Materialia*[J], 2016, 112: 242
20 Wu X X, Dlouhy A, Eggeler Y M *et al*. *Acta Materialia*[J], 2018, 144: 642
21 Li Y F, Wang L, Zhang G *et al*. *Materials Science and Engineering A*[J], 2019, 763: 138162
22 Yu J, Li J R, Shi Z X *et al*. *Advanced Materials Research*[J], 2012, 535–537: 888
23 Liu W W, Liu S Z, Li J R *et al*. *Materials Research Innovations*[J], 2014, 18(S4): 445

24 Li J R, Liu S Z, Wang X G *et al*. *Superalloys 2016: Proceedings of the 13th International Symposium of Superalloys*[C]. Seven Springs: The Minerals, Metals & Materials Society, 2016: 57

25 Hino T, Kobayashi T, Koizumi Y *et al*. *Superalloys 2000: Proceedings of the 9th International Symposium of Superalloys*[C]. Beppushi: The Minerals, Metals & Materials Society, 2000: 729

26 Jin Tao, Zhou Yizhou, Wang Xinguang *et al*. *Acta Metallurgica Sinica*[J], 2015, 51(10): 1153 (in Chinese)

27 Xia W S, Zhao X B, Yue L *et al*. *Journal of Alloys and Compounds*[J], 2020, 819: 152954

28 Yue Quanzhao. *Elevated Temperature Creep Behavior and Mechanism of the Third-Generation Ni-based Single Crystal Superalloy DD33*[D]. Xi'an: Northwestern Polytechnical University, 2019 (in Chinese)

29 Murakumo T, Koizumi Y, Kobayashi K *et al*. *Superalloys 2004: Proceedings of the 10th International Symposium of Superalloys*[C]. Austin: The Minerals, Metals & Materials Society, 2004: 155

30 Field R D, Pollock T M, Murphy W H. *Superalloys 1992: Proceedings of the 7th International Symposium of Superalloys*[C]. Seven Springs: The Minerals, Metals & Materials Society, 1992: 557

31 Argon A S. *Strengthening Mechanisms in Crystal Plasticity*[M]. Oxford: Oxford University Press, 2007

32 Alexander E, Thomas L, Hellmuth K *et al*. *Materials at High Temperatures*[J], 2014, 27(1): 53

33 Cheng Yuan, Zhao Xinbao, Yue Quanzhao *et al*. *Rare Metal Materials and Engineering*[J], 2023, 52(7): 2599 (in Chinese)

34 Yuan Y, Kawagishi K, Koizumi Y *et al*. *Materials Science and Engineering A*[J], 2014, 680: 95

35 Zhang J X, Murakumo T, Harada H *et al*. *Superalloys 2004: Proceedings of the 10th International Symposium of Superalloys*[C]. Austin: The Minerals, Metals & Materials Society, 2004: 189

36 Koizumi Y, Kobayashi T, Yokokawa T *et al*. *Superalloys 2004: Proceedings of the 10th International Symposium of Superalloys*[C]. Austin: The Minerals, Metals & Materials Society, 2004: 35

37 Zhao Jie, Ye Fei, Wang Qing. *Fundamentals of Materials Science*[M]. Dalian: Dalian University of Technology Press, 2015 (in Chinese)

38 Yue Quanzhao, Liu Lin, Yang Wenchao *et al*. *Materials Reports*[J], 2019, 33(3): 479 (in Chinese)

39 He C, Liu L, Huang T *et al*. *Vacuum*[J], 2020, 183: 109839

40 Fan Y S, Huang W Q, Yang X G *et al*. *Materials Science and Engineering A*[J], 2019, 757: 134

41 Reed R C. *The Superalloys: Fundamentals and Applications*[M]. Beijing: China Machine Press, 2016

42 Li Jiarong, Xiong Jichun, Tang Dingzhong. *Advanced High Temperature Structural Materials and Technology*[M]. Beijing: National Defense Industry Press, 2012 (in Chinese)

43 Tan Z H, Wang X G, Du Y L *et al*. *Materials Science and Engineering A*[J], 2020, 7: 138997

44 Huang Ming. *Creep Strengthening Mechanism in Re-doping Nickel-Based Single Crystal Superalloy and Defect Structure in Single Crystal Blades*[D]. Beijing: Tsinghua University, 2015 (in Chinese)

45 Long Haibo. *The Microstructural Evolution and Regulation of Ni-based Single Crystal Superalloy During High Temperature and Low Stress Creep Condition*[D]. Beijing: Beijing University of Technology, 2019 (in Chinese)

46 He J Y, Cao L J, Makineni S K *et al*. *Scripta Materialia*[J], 2021, 191: 23

DD9合金在蠕变过程中的组织演变

王　锐，李嘉荣，岳晓岱，赵金乾，杨万鹏

(北京航空材料研究院 先进高温结构材料重点实验室，北京 100095)

摘　要：对单晶高温合金DD9在980 ℃/250 MPa和1100 ℃/137MPa条件下进行了蠕变中断与断裂试验。通过扫描电镜、透射电镜分析了蠕变过程中的微观组织演变。结果表明：在980 ℃/250 MPa和1100 ℃/137MPa蠕变条件下，合金的微观组织演变过程类似。弥散分布于γ基体中的立方状γ′相逐渐演化成垂直于应力方向的层状结构。γ基体通道平行于应力方向的宽度在蠕变过程中逐渐增加。γ基体通道宽度的增加与应变之间的关系在对数形式下满足线性关系，即γ基体宽度可以通过应变来推断，这可能为研究单晶高温合金在高温低应力蠕变过程中γ基体的宽度变化提供了一种方法。在蠕变早期，γ相中形成的位错首先通过交滑移在γ/γ′界面形成相互垂直的位错网，随后在高温下，外部应力和错配应力的耦合作用使得位错网演变为稳定的六边形态。在蠕变后期，位错剪切γ′相，直至试样断裂。

关键词：单晶高温合金；DD9；蠕变；组织演变；位错

作者简介：王　锐，男，1994年生，博士生，北京航空材料研究院先进高温结构材料重点实验室，北京 100095，电话：010-62498309，E-mail：WR0608@126.com